Atomic Structure of the β-SiC(100)-(3 × 2) Surface

F. Semond,[1] P. Soukiassian,[1] A. Mayne,[2] G. Dujardin,[2] L. Douillard,[1] and C. Jaussaud[3]
[1]*Commissariat à l'Energie Atomique, DSM-DRECAM-SRSIM, Centre d'Etudes de Saclay, Bâtiment 462, 91191 Gif sur Yvette Cedex, France*
and Département de Physique, Université de Paris-Sud, 91405 Orsay Cedex, France
[2]*Laboratoire de Photophysique Moléculaire, Université de Paris-Sud, Bâtiment 213, 91405 Orsay Cedex, France*
[3]*LETI (CEA-Technologies Avancées), DMEL, CEN/G, 85 X, 38041 Grenoble Cedex, France*
(Received 22 May 1996)

We investigate single domain β-SiC(100)-(3 × 2) surfaces (Si rich) by atom resolved scanning tunneling microscopy (filled and empty electronic states). Flat and high-quality surfaces having a low density of defects are grown with first identification of individual Si atoms and dimers. Si-Si dimers form rows perpendicular to the dimer direction in a (3 × 2) atomic arrangement with clear evidence of asymmetric dimers all tilted in the same direction (i.e., not anticorrelated). Several types of defects are identified including primarily missing dimers and dimer pairs. Addition Si is grown epitaxially with two-dimensional island formation having the (3 × 2) reconstruction. [S0031-9007(96)01102-7]

PACS numbers: 68.35.Bs, 81.65.–b

Because of its very interesting properties, silicon carbide (SiC) is a very suitable material for high frequency, high power, or high temperature electronic devices. In fact, this "refractory" IV-IV compound semiconductor is able to operate at elevated temperatures (≈600 instead of 150 °C, e.g., for silicon) [1]. In addition, due to very close lattice parameters, SiC is a most promising substrate for heteroepitaxial growth of group III nitrides. All these interesting features are driving forces in the recent fast growing interest in SiC surfaces and interfaces [2–10]. SiC is not a fully covalent semiconductor (unlike Si), with a significant charge transfer from Si to C, and exists in two different crystallographic structures, hexagonal (α) and cubic (β). The latter one is generally grown on a Si(100) wafer by chemical vapor deposition (CVD) which provides single crystalline β-SiC(100) thin films (few μm thick). However, in part due to the very large mismatch between SiC and Si lattice parameters (≈20%), this approach generally results in rough surfaces and interfaces with a large density of defects [8]. Depending on surface composition, the existence of various surface reconstructions has been established with the 3 × 2 corresponding to a Si-rich terminated surface [2–5]. The β-SiC(100) surface structure has been studied using various experimental techniques including primarily electron diffraction [2–8]. As pointed out recently [3], scanning tunneling microscopy (STM) did not so far resolve β-SiC surface fine detail structures, likely due to difficulties encountered in surface preparation [3,8]. In fact, in β-SiC(100)-(3 × 2) surface STM studies (filled electronic states only), no atom identification was achieved [7,8], with the smallest STM features assigned to two dimers parallel to rows at a 2/3 silicon surface coverage [7]. In contrast, medium energy ion scattering (MEIS) and reflection high energy electron diffraction (RHEED) experiments suggested a 1/3 surface silicon coverage [5]. The accurate knowledge and control of β-SiC(100) reconstructions, for which metal or insulator interface formation was lately shown to be very reconstruction specific [9], are mandatory in monitoring and understanding their properties.

In this Letter, we present an atom resolved β-SiC(100)-(3 × 2) STM investigation. High-quality and flat single domain β-SiC(100)-(3 × 2) surfaces having a low defect density are grown by Si deposition with surplus silicon leading to the formation of large two-dimensional Si islands exhibiting the 3 × 2 reconstruction. We bring the first identification of individual Si atoms and dimers shown to be asymmetric and all tilted in the same direction, and forming rows perpendicular to the dimers. Different types of defects are identified, including primarily missing dimers and paired dimers.

The experiments are performed at Laboratoire de Photophysique Moléculaire, Université de Paris-Sud/Orsay using an Omicron STM at a working pressure always better than 5×10^{-11} torr. All STM topographs, which were obtained by tunneling into filled and empty electronic orbitals by changing the tip-to-sample bias polarity, are very reproducible and not tip dependent. We use single domain SiC thin films (1 μm thick) prepared at LETI (CEA-Technologies Avancées) by C_3H_8 and SiH_4 CVD growth on vicinal (4°) Si(100) wafers. Surface contaminants (native oxide and carbon clusters) are removed by thermal annealings which also results in selective Si surface depletion. The Si stoichiometry is restored by room temperature Si deposition followed by thermal annealings at 1000 °C. The surface quality is checked by low energy electron diffraction (LEED) to give sharp 3 × 2 patterns. The ability of this method to achieve very reproducible and clean β-SiC(100)-(3 × 2) surfaces has also been checked independently by specific valence band and core level spectral features in photoemission spectroscopy using synchrotron radiation [4,9].

We first look at a large area of the β-SiC(100)-(3 × 2) surface. Figure 1 displays an 800 × 800 Å STM

topograph (filled states) which shows a long range order with a flat and well ordered surface having a low density of defects. Also of interest is the existence of a large terrace together with rectangular islands covering part of the surface. All these features have the same structure made of spot rows all in the same direction. This indicates that, when the 3×2 reconstruction is achieved, additional Si can still be epitaxially grown which indicates that, here, the Si growth on the 3×2 surface reconstruction is not self-limited [7,10]. The height above the surface of both islands and terrace are the same ($\approx$2.5 Å) which suggests that islands and terraces are correlated and belong to the same Si layer, with relative island sizes depending on Si deposition and thermal annealing sequences. Interestingly, the spot rows keep the same orientation on terraces and islands, suggesting double atomic height steps (in agreement with the value measured at 2.5 Å) as for the Si(100)-(2×1) surface [11].

Additional insights about β-SiC(100)-(3×2) surface structure can be found in Fig. 2 which displays a more detailed 400×400 Å STM topograph (filled states). Figure 2 shows the best high surface quality at the atomic level [at a standard comparable to Si(100)-(2×1) [11–13], with a low density of defects. In fact, one can clearly see oval spot rows (see also Fig. 1) distant by $\approx$8.5 Å while the oval spots are separated by $\approx$6 Å within the row. These distances are very close to $3 \times a$ and $2 \times a$, respectively, in agreement with the observed 3×2 LEED pattern ("a" being the nonreconstructed surface primitive unit cell parameter of 3.08 Å). The most frequent type of defect results from the missing of an oval (mark A, Fig. 2) or more, leading sometimes to a complete missing row (as seen in Fig. 1). A second type of defect appears to be especially interesting: It corresponds to some ovals having a size larger than average (mark B). One should remark that the existence of this particular type of defect corresponds to the origin of oval row translation, giving an alternate type of ordering. Another type of defect (C, Fig. 2) corresponds to oval spots laterally shifted in a direction perpendicular to the row within the same row. A zoom image (a) of Fig. 2 shows a detailed picture of A and B defect types: One can clearly see that defect B includes two "components" corresponding to two oval spots that are closer ($1 \times a$ instead of $2 \times a$). This aspect is even best evidenced by a height profile [(b) in Fig. 2] along the xx' axis crossing defect B.

In order to identify the origin of oval spots forming rows that are observed by tunneling into the filled states (Figs. 1 and 2), we now look at a STM topograph obtained by tunneling into the empty states. Figure 3 displays a 200×200 Å topograph which shows empty states (3/4 top of the picture) and filled states (1/4 bottom of the picture) images. Interestingly, ovals (filled states) split into two clear spots when tunneling into the empty states. Empty state topographs are known to be sensitive to dangling bond orbitals associated with individual atoms [13]. This indicates that the spots observed here (empty states) correspond to Si atoms having dangling bonds. In

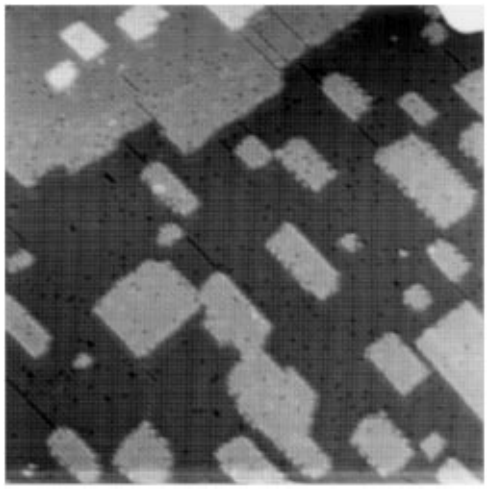

FIG. 1. β-SiC(100)-(3×2) surface 800 Å $\times$ 800 Å STM topograph (filled states). The tip bias was $V_t = +2.5$ V with a 0.2 nA tunneling current.

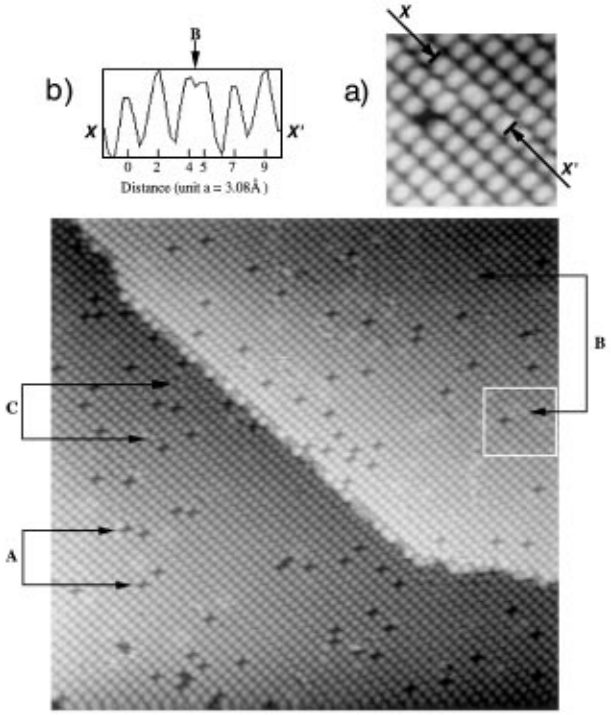

FIG. 2. β-SiC(100)-(3×2) surface 400 Å $\times$ 400 Å STM topograph (filled states). The different A, B, and C types of defects mentioned in the text are marked. The tip bias was $V_t = +2.5$ V with a 0.2 nA tunneling current. (a) Closeup of an area having type A (missing dimer) and B (dimer pair) defects. (b) Atomic profile of dimers along the xx' axis showing the two components of a dimer pair.

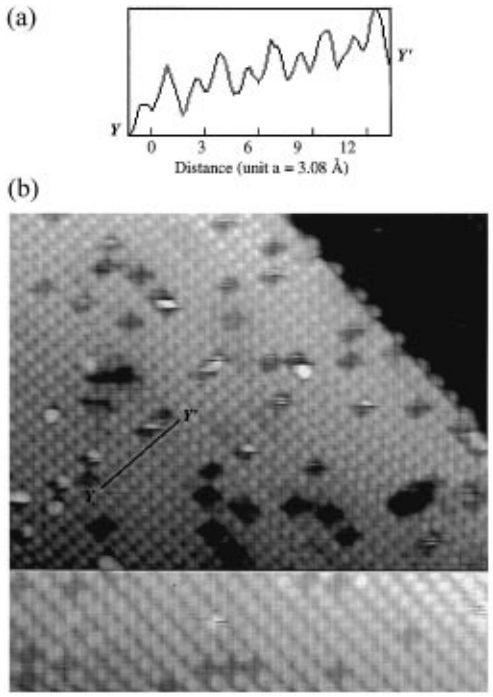

FIG. 3. β-SiC(100)-(3 $\times$ 2) surface 200 Å $\times$ 200 Å STM topograph obtained by tunneling into filled states (bottom) and empty states (top). The tip bias was $V_t = +3.5$ V with a 0.2 nA tunneling current. (a) Atomic profile of dimers along the yy' axis showing the height difference between two Si atoms belonging to the same dimer.

this view, the ovals (filled states) would then represent Si-Si dimers oriented perpendicularly to the rows. We also note a clear intensity difference between the two spots (empty states) related to a dimer (Fig. 3, top). Further confirmation of this crucial aspect is provided by a height profile along several dimers (yy' axis) perpendicular to dimer rows [Fig. 3(a)] which indicates best that the two atoms of a dimer do not have the same height. This very interesting feature shows that dimers are asymmetric and all tilted in the same direction (i.e., not alternate). While recently proposed in a theoretical study of β-SiC(100)-(3 $\times$ 2) [14], this finding has so far not been evidenced experimentally.

The assignment of an oval shape to a Si-Si dimer perpendicular to the row can be further supported by looking at defects B (Fig. 2), which mark the origin of rows displaced by a. The presence of such defects B can be readily explained by the displacement of a Si-Si dimer over a distance a along the row. In fact, from Fig. 2(a) and the height profile along the xx' axis [Fig. 2(b)], defect B presents two distinct ovals, i.e., indeed composed of two dimers that are closer and separated by a instead of "2 $\times$ a" in the normal row configuration. Defects B are labeled as "dimer pairs."

Additional support of the oval shape assignment to a single Si-Si dimer can be found by exploring the effect, at the atomic scale, of an oxygen exposure. Figure 4 displays STM topograph (filled states) of the same β-SiC(100)-(3 $\times$ 2) surface, respectively, for clean (top) and exposed to a very small amount of oxygen at 0.5 Langmuir (L) (bottom). At such a low oxygen exposure, one can expect to have only very few individual interactions between oxygen and silicon atoms. These are marked by arrows (Fig. 4), where it appears that the corresponding oval spots become separated into half-dark and half-light spots upon oxygen exposure. Although the exact assignment of the oxygen containing sites is not discussed here, this feature can be explained by oxygen interaction with a Si atom belonging to a dimer which further supports interpretation of the oval shape to a Si-Si dimer.

Our STM results show that, unlike general belief, high-quality and flat cubic silicon carbide surfaces having a low density of defects can be prepared, despite the CVD growth method and large lattice parameter mismatch ($\approx$20%) between the epitaxial SiC film and the substrate (Si). This low defect density, which meets the standard achieved for Si(100)-(2 $\times$ 1) surfaces [12,13], is likely to result from the appropriate sequences of Si deposition and thermal annealing. Our results provide a model of the

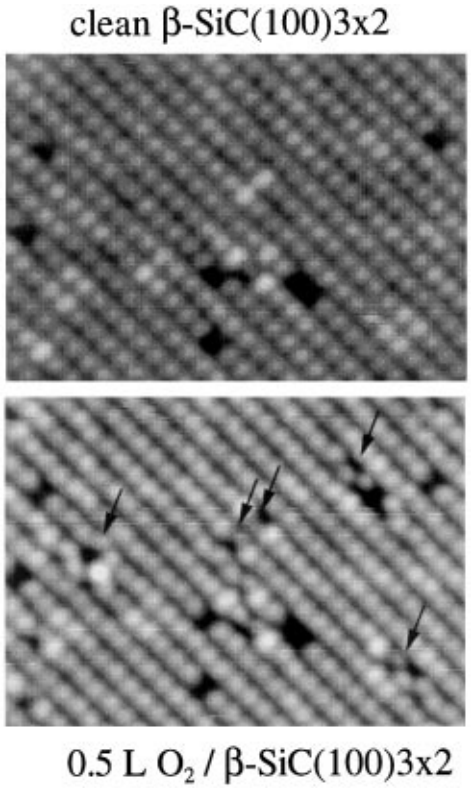

FIG. 4. Clean β-SiC(100)-(3 $\times$ 2) (top) and covered by 0.5 L of O_2 (bottom) surfaces 100 Å $\times$ 150 Å STM topograph obtained by tunneling into the filled states. The tip bias was $V_t = +3.5$ V with a 0.2 nA tunneling current. Arrows indicate some STM characteristic changes after O_2 deposition.

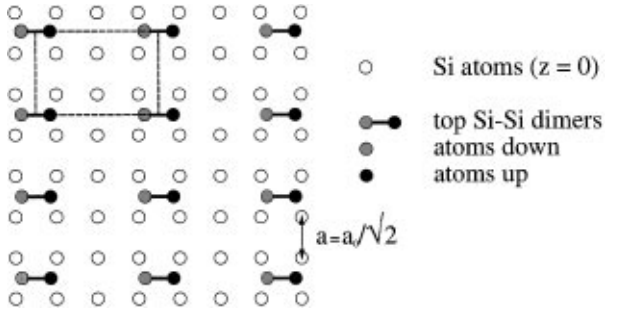

FIG. 5. Schematic of the 3×2 Si-Si dimer ordering on a nonreconstructed β-SiC(100) surface. The surface primitive unit cell parameter is $a = a_0/\sqrt{2}$, where $a_0 = 4.36$ Å is the β-SiC lattice constant. The dashed line represents the 3×2 unit cell.

β-SiC(100)-(3×2) surface in which oval spots represent individual Si-Si dimers oriented perpendicularly to the rows and separated by $2 \times a$. These dimers are found to be asymmetric and all in the same direction (i.e., not anticorrelated) (Fig. 5). This atomic configuration leaves a very open surface with dimers occupying, within a row, one possible site out of two.

The defects that are most commonly observed result from missing dimers (type *A* in Fig. 2), while another interesting type of defect (*B* in Fig. 2) is shown to correspond to two Si-Si dimers distant by only $1 \times a$. While defects *A*, which could form a complete missing dimer row (see Fig. 1), do not alter the atomic ordering, defects *B* are at the origin of dimer row shifts (along the row) by $1 \times a$, giving an alternate dimer row arrangement (Figs. 2 and 3). The present model (Fig. 5) gives a Si coverage of $1/3$, in contrast with conclusions drawn from the previous STM study [7], where a coverage of $2/3$ was inferred with pairs of Si dimers oriented parallel to the rows. Our model is based on the clear identification of individual Si atoms from the empty states topograph (Fig. 3). In addition, defects *B* are not consistent with a model of dimers oriented along the rows as proposed elsewhere [2,7]. Instead, defects *B* are easily explained in terms of a pair of dimers separated by $1 \times a$ (instead of $2 \times a$) as shown above. Therefore, our real-space observation of Si coverage of $1/3$ is in excellent agreement with models based on diffusion or diffraction techniques as MEIS and RHEED [5].

Another interesting feature is *C* type defects (Fig. 2) showing a lateral displacement (perpendicularly to the dimer row) of an oval spot. This suggests that corresponding dimers have a different tilt angle coming, in some cases, to an alternate asymmetric dimer configuration. *C* type defects seem to influence the neighboring atoms' short range order. Finally, Si islands are also of special interest since they exhibit the same 3×2 reconstruction as for ground surface with dimer rows keeping the same orientation. The presence of these Si islands demonstrates that the surface is not Si saturated after completion of the 3×2 reconstruction.

In conclusion, we have investigated β-SiC(100)-(3×2) by atom resolved STM (filled and empty electronic states) showing high-quality surfaces with a low defect density. Individual Si atoms and dimers are identified with asymmetric dimer formation all tilted in the same direction (i.e., not alternate tilting) and forming rows perpendicular to the dimer leaving a very open atomic surface arrangement. Three types of defects are identified, including missing dimers, dimer pairs, and also some few dimers having different tilt angles. Additional Si could be grown epitaxially with large islands having also the (3×2) reconstruction. This work brings novel and deep insights into the knowledge of technologically important silicon carbide atomic surface structure.

[1] R. F. Davis, J. Vac. Sci. Technol. A **11**, 829 (1993).
[2] M. Dayan, J. Vac. Sci. Technol. A **4**, 38 (1986); R. Kaplan, Surf. Sci. **215**, 111 (1989).
[3] R. Kaplan and V. M. Bermudez, in *Properties of Silicon Carbide*, edited by G. Harris, EMIS Datareview Series Vol. 13 (INSPEC, London, 1995), p. 101.
[4] V. M. Bermudez and J. P. Long, Appl. Phys. Lett. **66**, 475 (1995).
[5] S. Hara, W. F. J. Slijkerman, J. F. van der Veen, I. Ohdomari, S. Misawa, E. Sakuma, and S. Yoshida, Surf. Sci. Lett. **231**, L196 (1990); T. Yoshinobu, I. Izumikawa, H. Mitsui, T. Fuyuki, and H. Matsunami, Appl. Phys. Lett. **59**, 2844 (1991).
[6] J. P. Long, V. M. Bermudez, and D. E. Ramaker, Phys. Rev. Lett. **76**, 991 (1996).
[7] S. Hara, S. Misawa, S. Yoshida, and Y. Aoyagi, Phys. Rev. B **50**, 4548 (1994).
[8] C. S. Chang, N. J. Zheng, I. S. T. Tsong, Y. C. Wang, and R. F. Davis, J. Am. Ceram. Soc. **73**, 3264 (1990); J. Vac. Sci. Technol. B **9**, 681 (1991).
[9] F. Semond, L. Douillard, P. Soukiassian, D. Dunham, F. Amy, and S. Rivillon, Appl. Phys. Lett. **68**, 2144 (1996); F. Semond, P. Soukiassian, P. S. Mangat, Z. Hurych, L. di Cioccio, and C. Jaussaud (to be published); M. Riehl-Chudoba, P. Soukiassian, C. Jaussaud, and S. Dupont, Phys. Rev. B **51**, 14 300 (1995).
[10] S. Hara, Y. Aoyagi, M. Kawai, S. Misawa, E. Sakuma, and S. Yoshida, Surf. Sci. **273**, 437 (1992).
[11] P. E. Wierenga, J. A. Kubby, and J. E. Griffith, Phys. Rev. Lett. **59**, 2169 (1987).
[12] B. S. Swartzentruber, Y. W. Mo, M. B. Webb, and M. G. Lagally, J. Vac. Sci. Technol. A **7**, 2901 (1989).
[13] P. Bedrossian, Phys. Rev. Lett. **74**, 3648 (1995).
[14] H. Yan, A. P. Smith, and H. Jónsson, Surf. Sci. **330**, 265 (1995).